Microstructures in solids: their critical role in governing material mechanical behavior

Katia Bertoldi

Multi Scale Mechanics, University of Twente, The Netherlands

September 22nd, 08

1

Novel and optimal materials at small scales, e.g. **nano-composites** and **biological composites**, characterized by

- excellent mechanical properties;
- morphology tailored to enable wide range of macroscopic level functions.

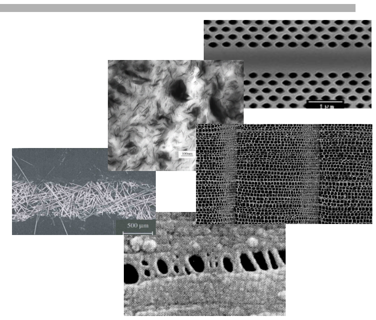

Mechanical characterization of their **microstructure**

↓

Micromechanical models

↓

Macroscopic constitutive equations

↓

Explanation and better understanding of the **experimental results**

2

My research goal:
The establishment of the relationships between **topology**, **material properties** and **performance**

Material properties

Structure ↔ **Performance**

- It allows us to **use the materials to "their full potential"**
- It allows us to **design better materials**.

Research projects

Micromechanics-based development of macroscopic constitutive equations for

- **Lattice structures**

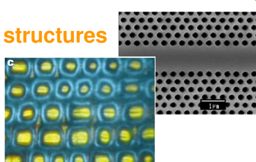

- **Mussel Byssus**

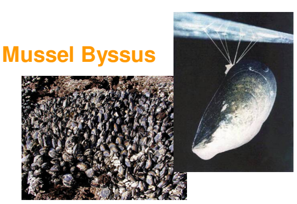

- **EMAA**

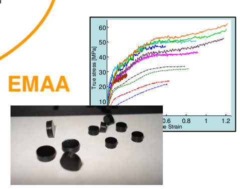

- **Structural interfaces**

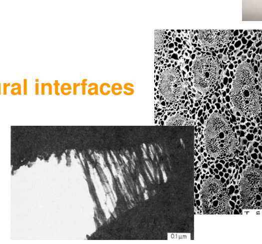

- **Bridged cracks**

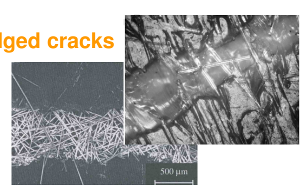

Mechanics of Deformation-Triggered Pattern Transformation in Periodic Elastomeric Structures

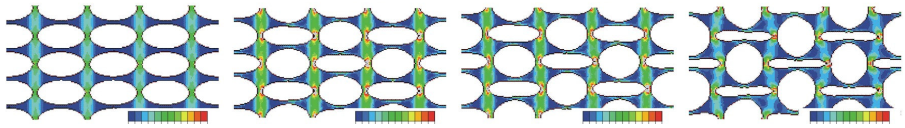

- The application of a simple load to a periodic structure can trigger an **unexpected global pattern switch above a critical point**. The results of numerical investigations reveal that the pattern switch is triggered by a **reversible elastic instability**
- Possibility of **creating prescribed complex patterns** on currently available periodic lattices
- Possibility of **switching certain properties on and off with deformation**

Outline

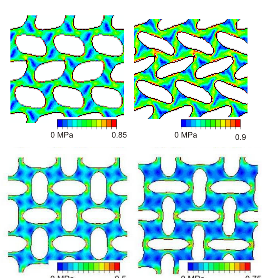

Experimental results
Compression tests of specimens with periodic lattice microstructure

Modeling
- **Analyses of instabilities**
  - Eigen value analyses on finite sized specimens
  - Refined Eigen analyses on periodic RVEs
  - Bloch Wave analyses on primitive cell
  - Loss of ellipticity analyses on primitive cell
- **Post-transformation analyses**
  - Simulations of compression tests
- **Transformations of Phononic Band Gaps**

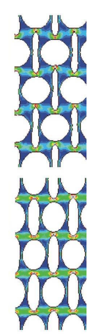

Mullin, Deschanel, Bertoldi, Boyce
"Pattern transformation triggered by deformation", *Physical Review Letters 99, 2007, 084301*.

Bertoldi, Boyce, Deschanel, Prange, Mullin
"Mechanics of deformation-triggered pattern transformations and superelastic behavior in periodic elastomeric structures", *JMPS 2008*

Bertoldi, Boyce
"Mechanically-Triggered Transformations of Phononic Band Gaps in Periodic Elastomeric Structures", *Physical Review B 2008*

Lattice structures

Increasing interest for the creation and use of **nano- and micron-scale periodic structures** to achieve unique properties.

Photonic crystals designed to affect the propagation of electromagnetic waves.

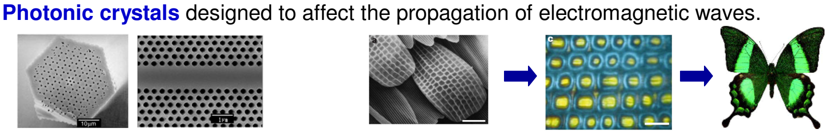

Applications: LEDs, optical fibers, nanoscopic lasers, radio frequency antennas

Phononic crystals ➡ effects of their periodic structure on wave propagation

Applications: sound filters, transducer design and acoustic mirrors.

Super-hydrophobic surfaces ➡ Micro-textures that modify the material wettability

Periodic structures under investigation

We manufactured **2D lattice cellular structures (at the millimeter length-scale) from elastomeric sheets**

Finite sized specimens

Circular holes on a square lattice | **Elliptical holes on a rectangular lattice** | **Circular holes on an oblique lattice**

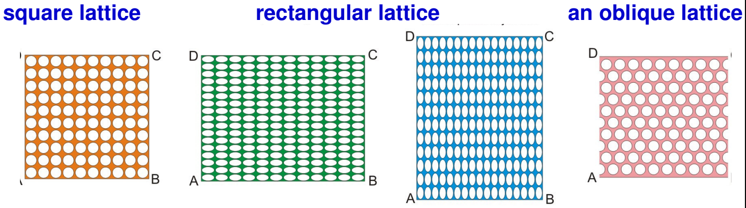

Infinite periodic structures

Primitive cell
(Bloch wave analysis)

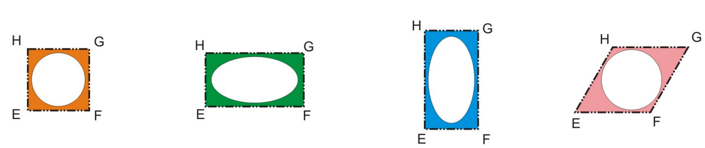

University of Twente
The Netherlands

Experimental results: Circular holes on a square lattice

Uniaxial Compression tests

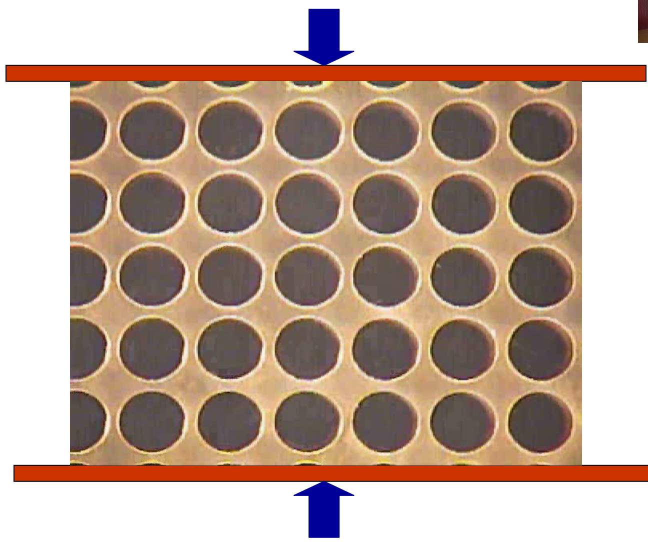

University of Twente
The Netherlands

Experimental results: Circular holes on a square lattice

Compression tests

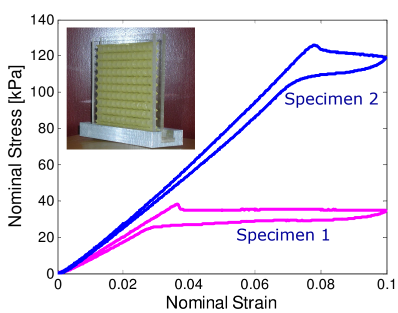

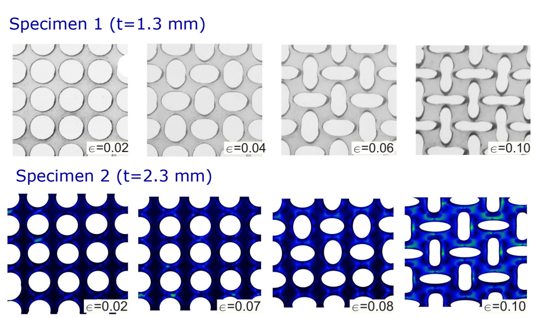

- Initial linear elastic behavior with a sudden departure from linearity to a plateau stress
- **Completely homogeneous pattern transformation** ➡ corresponds to the plateau region
- **The transformed pattern is accentuated** with continuing deformation
- The critical triggering stress level scales consistently with **ligament buckling**

Experimental results: Rectangular lattice of elliptical holes

Compression tests

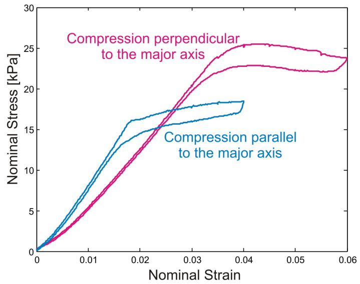

Uniaxial compression in directions parallel and perpendicular to the major axis of the holes

- Initially **linear stress-strain behavior**

- Then **the stress plateaus as a result of the pattern transformation**

The transformation is a result of a local instability: **reversible and repeatable pattern transformation**

Compression perpendicular to the major axis

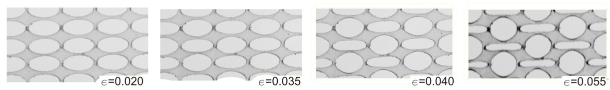

Compression parallel to the major axis

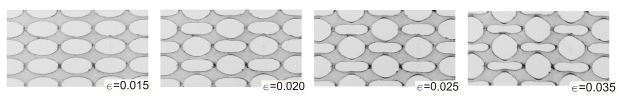

11

University of Twente
The Netherlands

Experimental results: Oblique lattice of circular holes

Compression tests

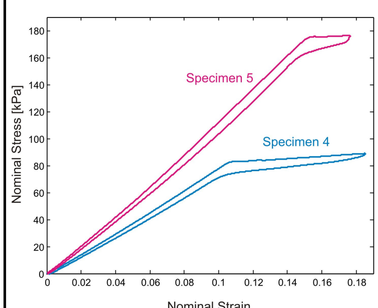

Specimen 4

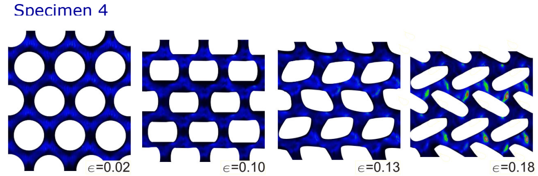

- The pattern transformation is a result of a **critical intervoid shear instability event**.

- The pattern after transformation is one of **sheared voids** where the shear direction alternates back and forth from row to row.

12

Modeling

Experimental results suggest that the **pattern transformation** is the result of an **elastic instability** in the inter-hole ligaments

The finite sized specimens are influenced by boundary conditions ➡ the deformation behavior of **infinite periodic structures** is also modeled.

- **Finite Sized Specimen**
  - Instability via **Eigen Value Analyses**
  - **Stress-Strain Behavior**

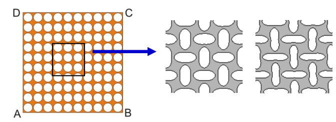

Infinite periodic structures

- **Primitive Cells**
  - Microscopic Instability via **Bloch Wave Analysis**
  - Macroscopic Instability via **Loss of ellipticity**

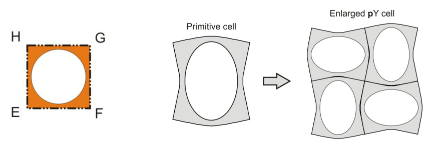

- **Periodic Multicell RVEs**
  - **Stress-Strain Behavior**

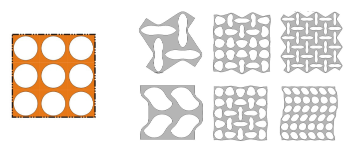

Elastomeric material behavior

Uniaxial compression stress-strain tests to characterize the material response of the elastomeric matrix.

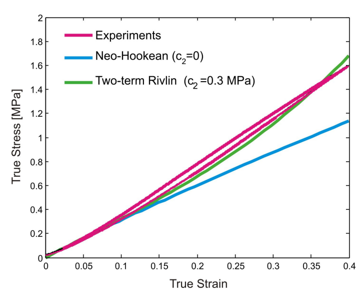

Material exhibits a behavior typical for elastomers: large strain elastic behavior with **negligible rate dependence and negligible hysteresis**

Strain energy density for an isotropic hyperelastic material

$$W = W(I_1, I_2, I_3)$$

The PSM-4 stress-strain behavior is modeled using a **two-term I1-based Rivlin model** (modified to include compressibility)

$$W(I_1, I_3) = c_1(I_1 - 3) + c_2(I_1 - 3)^2 - 2c_1 \log J + \frac{K}{2}(J-1)^2$$

C_1=0.55 MPa
C_2=0.3 MPa

Cauchy stress

$$\boldsymbol{\sigma} = \frac{2}{J}\left[c_1 + 2c_2(I_1 - 3)\right]\boldsymbol{B} + \left[K(J-1) - 2\frac{c_1}{J}\right]\boldsymbol{I}$$

Boundary conditions

- **Finite-sized periodic structure**

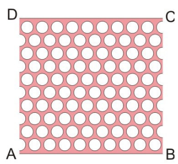

Bottom edge AB is fixed in vertical direction

Top edge CD is uniformly compressed in vertical direction

- **Infinite periodic structure**

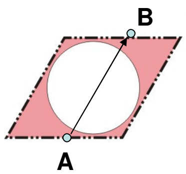

Periodic boundary conditions on the cell boundaries

$$\mathbf{u}|_B - \mathbf{u}|_A = (\bar{\mathbf{F}} - \mathbf{I})[\mathbf{X}|_B - \mathbf{X}|_A] = \bar{\mathbf{H}}\,[\mathbf{X}|_B - \mathbf{X}|_A],$$

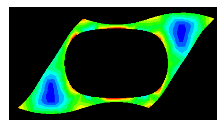

Macroscopic uniaxial compression

$$\bar{\mathbf{H}} = \bar{H}_{11}\,\mathbf{e}_1 \otimes \mathbf{e}_1 + (\lambda - 1)\,\mathbf{e}_2 \otimes \mathbf{e}_2$$

- Components of $\bar{\mathbf{H}}$ are viewed as generalized degrees of freedom (operationally applied using a set of virtual nodes).

- The **macroscopic first Piola-Kirchoff stress tensor** and the corresponding macroscopic Cauchy stress tensor are then extracted through virtual work considerations

Danielsson M., Boyce M.C., Parks D.M., JMPS 2002 and 2007

15

Analysis of instabilities: Eigen Analysis

A **linear perturbation procedure** is used

ABAQUS/Standard

- **Finite-sized periodic structure: Square array of circular holes**

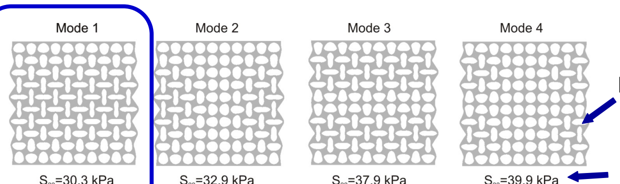

Same pattern as in the experimental tests

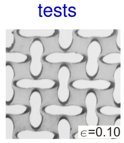

Experiments

Pattern transformation

Result of elastic instability

16

Analysis of instabilities: Bloch wave Analysis

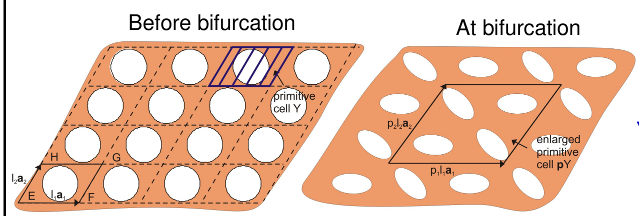

Bifurcation
⬇
Y-periodicity may break down
(enlarged primitive cell **p**Y)

The **primitive cell** Y is considered together with **velocities** given by the **Bloch** type relation

$$\mathbf{v}(\mathbf{X} + l_j \mathbf{a}_j) = \mathbf{v}(\mathbf{X}) \exp[i \mathbf{k}_0 \cdot (l_j \mathbf{a}_j)], \quad j=1,2$$

Complex-valued function

$\mathbf{k}_0$ lying in the unit cell of the reciprocal lattice

Triantafyllidis N., Nestorovic, M.D., Schraad M.W., J. Applied Mech. 2006

Analysis of instabilities: Bloch wave Analysis

Aberg M., Gudmundson P., J. Acoust. Soc. Am. 1997

ABAQUS does not directly handle complex valued displacements

• All the **fields** are split into a **real and imaginary parts**

• **Two uncoupled set of equilibrium equations** (one for the real and one for the imaginary part) are obtained

• The problem is solved using **two identical finite element meshes** for the primitive cell, one for the real part and one for the imaginary part, **coupled by the Bloch type displacement boundary conditions**

• Finite element discretization

$$\begin{bmatrix} \mathbf{K} & 0 \\ 0 & \mathbf{K} \end{bmatrix} \begin{bmatrix} \hat{\mathbf{v}}^{\mathrm{Re}} \\ \hat{\mathbf{v}}^{\mathrm{Im}} \end{bmatrix} = \begin{bmatrix} \dot{\mathbf{f}}^{\mathrm{Re}} \\ \dot{\mathbf{f}}^{\mathrm{Im}} \end{bmatrix},$$

The stiffness matrix **K** is obtained from ABAQUS

• Application of **boundary conditions** and **static condensation** of the degrees of freedom belonging to the nodes on the edges HG and FG

$$\tilde{\mathbf{K}} \begin{bmatrix} \hat{\mathbf{v}}_a^{\mathrm{Re}} \\ \hat{\mathbf{v}}_a^{\mathrm{Im}} \end{bmatrix} = \mathbf{0}, \qquad \tilde{\mathrm{K}} = \tilde{\mathrm{K}}(\lambda, \mathrm{k}_0)$$

Eigenvalue problem

Find the minimum load for which a vector $\mathbf{k}_0$ exists such that the lowest eigenvalue is equal to zero

Analysis of instabilities: Bloch wave Analysis

• **Infinite periodic structure: Square array of circular holes**

During compression simulations

• **a critical instability is detected at an engineering strain of - 0.03** with $k_{01}=1/(2\ l_1)$ and $k_{02}=1/(2\ l_2)$

• **Y-periodicity is broken** and an **enlarged cell** **p**Y with **p=(2,2)** is found $p_1 = \frac{1}{k_{01} l_1}, \quad p_2 = \frac{1}{k_{02} l_2}$

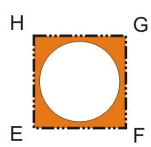

Primitive cell

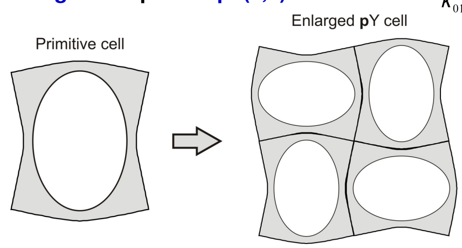

Eigen Mode of the microscopic bifurcation as predicted by the Bloch wave analysis

• After the 1st Eigen mode at an engineering **strain of -0.055 loss of ellipticity** for the homogenized tangent modulus is found, leading to a macroscopic instability

19

Results: Circular holes on a square lattice

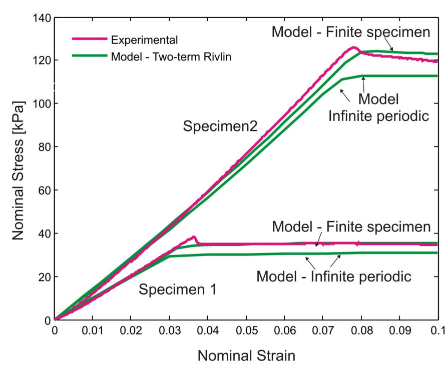

• **Excellent quantitative agreement** between experiments and simulations

• Infinite periodic solid earlier departure from linearity

• For the **two-terms Rivlin and the Neo-Hookean** material models **almost identical** stress-strain behavior

Experiments

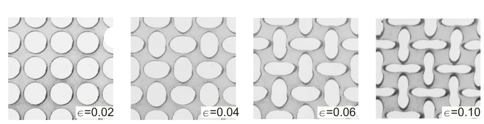

Simulations

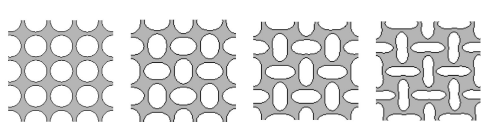

20

Pattern transformation

Application of a simple load to a periodic structure can trigger an **unexpected global pattern switch** above a critical point.

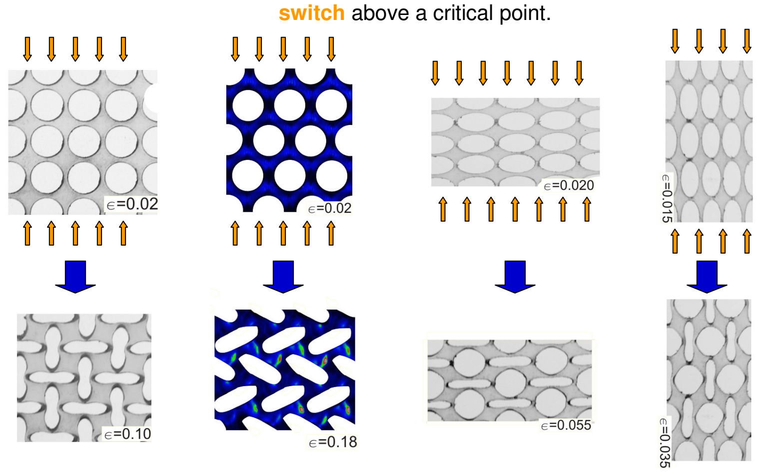

- Possibility of **creating prescribed complex patterns** on currently available periodic lattices
- Possibility of **switching certain properties on and off with deformation**

Phononic crystals

Phononic crystals ➡ periodic elastic structures with a **range in frequency where elastic wave propagation is barred** (band gap)

Applications: sound filters, acoustic wave guides and acoustic mirrors.

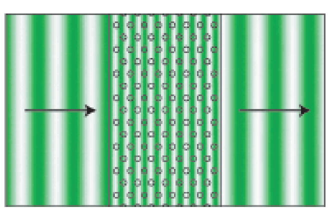

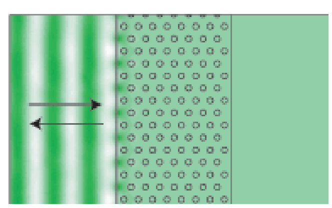

Pattern transformation ➡ Transformative Phononic band gaps materials

Wave propagation in periodic materials

Propagation of harmonic waves in a periodic hyperelastic material

Governing equations

$$\mathrm{Div}\dot{\mathbf{S}} = \rho_0 \frac{\partial^2 \mathbf{V}}{\partial t^2}, \qquad \dot{\mathbf{S}} = \mathbb{L} : \dot{\mathbf{F}}$$

The **solution** will be in the form

$$\mathbf{V}(\mathbf{X}, t) = \boldsymbol{\mathcal{V}}(\mathbf{X}) \exp[-\mathrm{i}\omega\, t], \quad \Rightarrow \quad \mathrm{Div}\dot{\boldsymbol{\mathcal{S}}} + \rho_0 \omega^2 \boldsymbol{\mathcal{V}} = 0.$$

complex valued function

The **velocities** are given by the **Bloch type** relation

$$\boldsymbol{\mathcal{V}}(\mathbf{X} + l_j \mathbf{a}_j) = \boldsymbol{\mathcal{V}}(\mathbf{X}) \exp[\mathrm{i}\mathbf{K}_0 \cdot (l_j \mathbf{a}_j)].$$

To work with the **complex valued displacements** of the Bloch wave calculation within ABAQUS

$$\boldsymbol{\mathcal{V}}(\mathbf{X}) = \boldsymbol{\mathcal{V}}(\mathbf{X})^{Re} + \mathrm{i}\boldsymbol{\mathcal{V}}(\mathbf{X})^{Im}$$

Two sets of uncoupled equations for the real and imaginary parts

$$\begin{cases} \mathrm{Div}\dot{\boldsymbol{\mathcal{S}}}^{Re} + \rho_0 \omega^2 \boldsymbol{\mathcal{V}}^{Re} = 0, \\ \mathrm{Div}\dot{\boldsymbol{\mathcal{S}}}^{Im} + \rho_0 \omega^2 \boldsymbol{\mathcal{V}}^{Im} = 0. \end{cases} \Leftarrow \quad \begin{aligned} \boldsymbol{\mathcal{V}}(\mathbf{X} + l_j \mathbf{a}_j)^{Re} &= \boldsymbol{\mathcal{V}}^{Re}(\mathbf{X}) \cos[\mathbf{K}_0 \cdot (l_j \mathbf{a}_j)] - \boldsymbol{\mathcal{V}}^{Im}(\mathbf{X}) \sin[\mathbf{K}_0 \cdot (l_j \mathbf{a}_j)] \\ \boldsymbol{\mathcal{V}}(\mathbf{X} + l_j \mathbf{a}_j)^{Im} &= \boldsymbol{\mathcal{V}}^{Re}(\mathbf{X}) \sin[\mathbf{K}_0 \cdot (l_j \mathbf{a}_j)] + \boldsymbol{\mathcal{V}}^{Im}(\mathbf{X}) \cos[\mathbf{K}_0 \cdot (l_j \mathbf{a}_j)] \end{aligned}$$

Aberg M., Gudmundson P., J. Acoust. Soc. Am. 1997

23

Wave propagation in periodic materials

Two identical finite element meshes for the RVE, one for the real part and one for the imaginary part and **coupling them by Bloch type displacement** boundary conditions

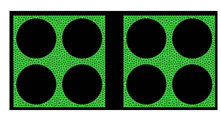

Finite element formulation

$$\left[\begin{pmatrix} [\mathrm{K}] & 0 \\ 0 & [\mathrm{K}] \end{pmatrix} - \omega^2 \begin{pmatrix} [\mathrm{M}] & 0 \\ 0 & [\mathrm{M}] \end{pmatrix} \right] \begin{bmatrix} \hat{\mathrm{v}}^{Re} \\ \hat{\mathrm{v}}^{Im} \end{bmatrix} = \begin{bmatrix} \hat{\mathrm{f}}^{Re} \\ \hat{\mathrm{f}}^{Im} \end{bmatrix}$$

Boundary conditions yield

$$\begin{bmatrix} \hat{\mathrm{v}}^{Re} \\ \hat{\mathrm{v}}^{Im} \end{bmatrix} = [\mathrm{Q}_v] \begin{bmatrix} \hat{\mathrm{v}}_i^{Re} \\ \hat{\mathrm{v}}_a^{Re} \\ \hat{\mathrm{v}}_i^{Im} \\ \hat{\mathrm{v}}_a^{Im} \end{bmatrix} \qquad \begin{bmatrix} \hat{\mathrm{f}}^{Re} \\ \hat{\mathrm{f}}^{Im} \end{bmatrix} = [\mathrm{Q}_f] \begin{bmatrix} \hat{\mathrm{f}}_i^{Re} \\ \hat{\mathrm{f}}_a^{Re} \\ \hat{\mathrm{f}}_i^{Im} \\ \hat{\mathrm{f}}_a^{Im} \end{bmatrix}$$

$[Q_v]=Q_v[k_0]$ **$[Q_f]=Q_f[k_0]$**

$$[\mathrm{Q}_v]^T \left[\begin{pmatrix} [\mathrm{K}] & 0 \\ 0 & [\mathrm{K}] \end{pmatrix} - \omega^2 \begin{pmatrix} [\mathrm{M}] & 0 \\ 0 & [\mathrm{M}] \end{pmatrix} \right] [\mathrm{Q}_v] \begin{bmatrix} \hat{\mathrm{v}}_i^{Re} \\ \hat{\mathrm{v}}_a^{Re} \\ \hat{\mathrm{v}}_i^{Im} \\ \hat{\mathrm{v}}_a^{Im} \end{bmatrix} = 0$$

Eigenfrequency

Eigenfrequencies ω can be computed for any Bloch-vector k_0

24

Circular holes on a square array

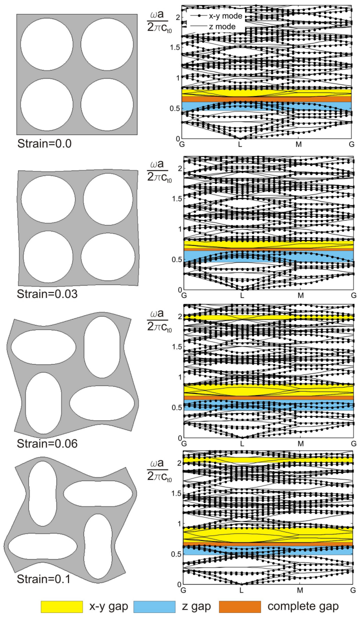

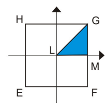

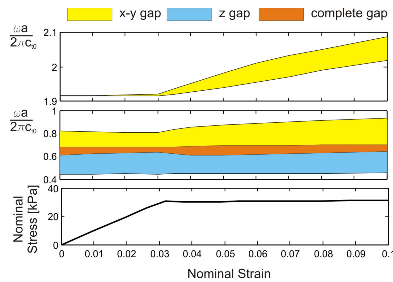

Initial linear response
Band gaps affected marginally by deformation, **evolving in an affine and monotonic way**

Pattern transformation
The **in-plane modes undergo a transformation**
- **a new band gap is opened**
- **the pre-existing band gap widens**

The out-of-plane modes are marginally affected

25

Nanoscale materials

In collaboration with:
Prof. Edwin L. **Thomas**, Institute for Soldier Nanotechnologies, MIT
Prof. Vladimir **Tsukruk**, Georgia Institute of Technology

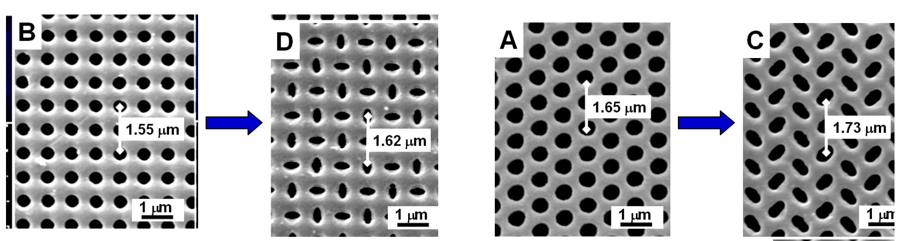

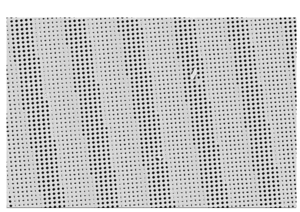

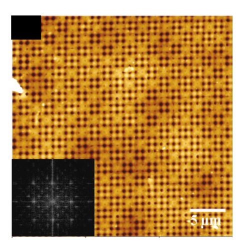

26

Conclusions

Novel, homogeneus and reversible pattern transformations have been uncovered

The pattern transformation induces a **non-affine change in the phononic band-gaps**

The pattern can be **switched on and off** ➡ phononic switch to allow or to prevent the transmission of certain elastic waves

Imprinting complex pattern during fabrication process ➡ elliptical patterns have a marked effect on the transmission of polarized light

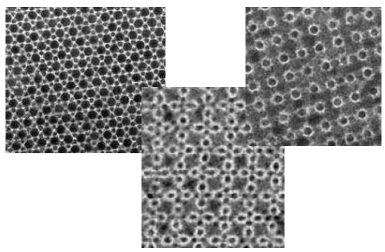

27

Thanks for your attention

28

Experimental results

Homogeneous pattern transformation

Circular holes on a square lattice

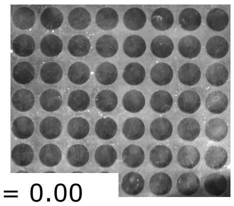

ε = 0.00

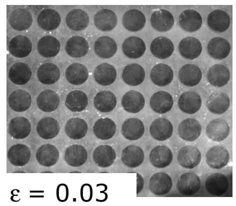

ε = 0.03

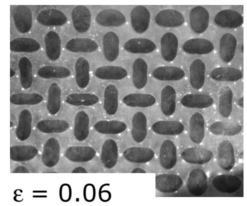

ε = 0.06

Circular holes on an oblique lattice

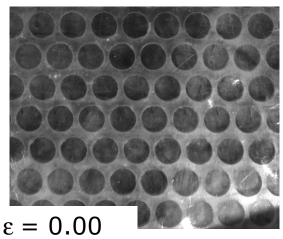

ε = 0.00

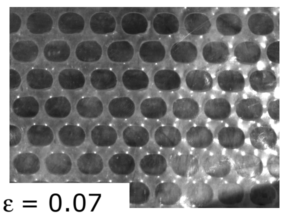

ε = 0.07

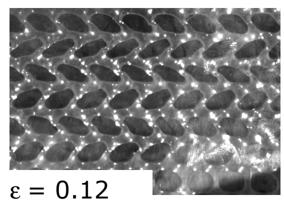

ε = 0.12

Circular hole on an oblique array

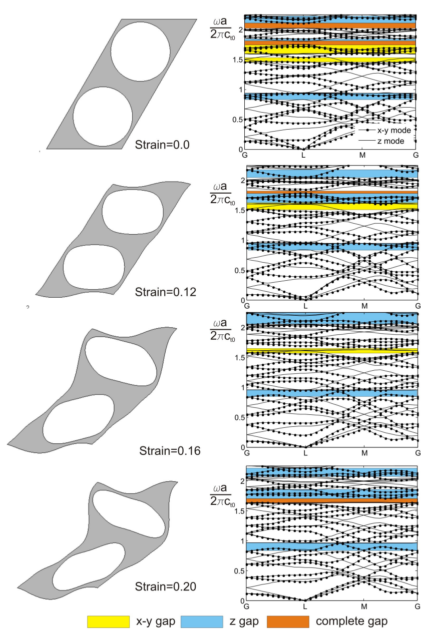

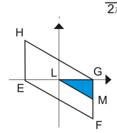

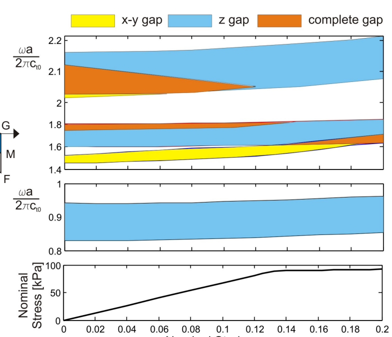

The **out-of-plane band gaps** are **marginally affected** by the pattern transformation

The **in-plane band gaps**
• the **lowest band gap** intersects the z-mode yielding a **complete band gap**
•The **2nd and 3rd band gaps close completely**

Transformative phononic band gaps

- Propagation of elastic waves through each structure is analyzed at **different levels of macroscopic strain**
- The finite element method (ABAQUS/Standard) is used to compute the **band structure**

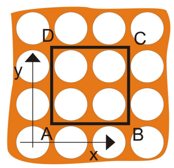

Circular holes on a square array

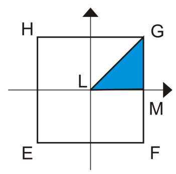

Reciprocal lattice

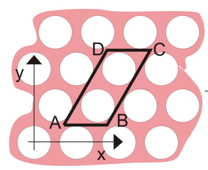

Circular holes on an oblique array

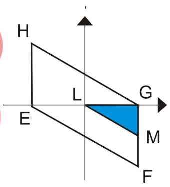

Reciprocal lattice

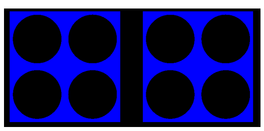

Undeformed

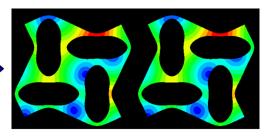

Deformed

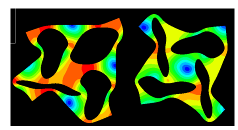

EigenFrequency analysis

Results: Circular holes on an oblique lattice

- **Finite-sized periodic structure**

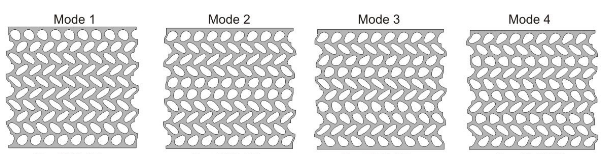

S_{22}=70.8 kPa | S_{22}=72.9 kPa | S_{22}=76.9 kPa | S_{22}=82.2 kPa

First mode ➡ same pattern as in the experimental test

- **Infinite periodic structure**

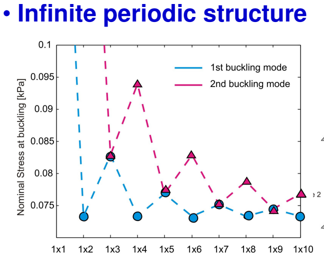

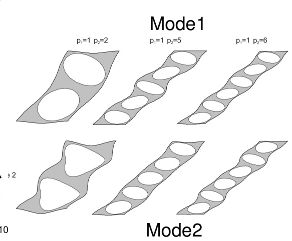

Refined Eigen Analyses
- All the RVEs with **1x 2m** primitive cells have the **same 1st Eigen mode**
- The **2nd Eigen mode decreases** increasing the RVE size, suggesting a "global" mode

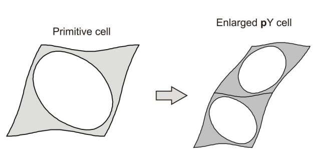

Bloch wave Analyses
- **At instability, enlarged primitive cell pY with p=(1,2)**
- After the 1st Eigen Mode, **loss of ellipticity** occurs

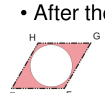

"global" Eigen Mode

Results: Circular holes on an oblique lattice

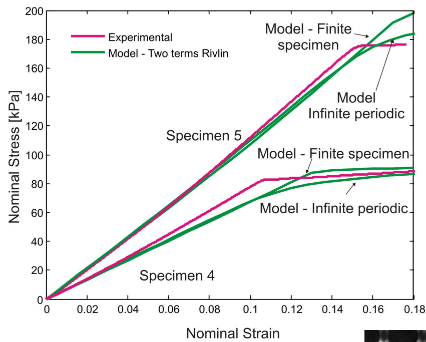

- **Excellent quantitative agreement** between experiments and simulations
- For the **two-terms Rivlin and the Neo-Hookean** material models **almost identical** stress-strain behavior

Experiments

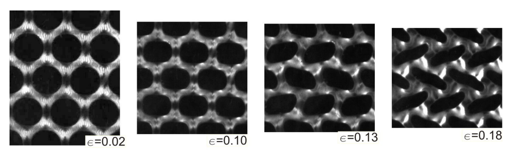

Simulations

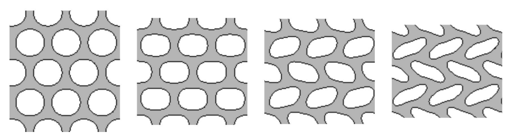

33

Analysis of instabilities: Eigen Analysis

- **Infinite periodic structure: Square array of circular holes**

- **Refined Eigen analyses on RVEs of increasing size** (**p**Y cells with **p**=(p_1,p_2)) subjected to periodic boundary conditions.

- **Each cell pY** is characterized by a critical value of the loading parameter λ^p**.** The critical value of the load parameter λ^{cr} is defined as the **infimum of λ^p on all possible cells pY**

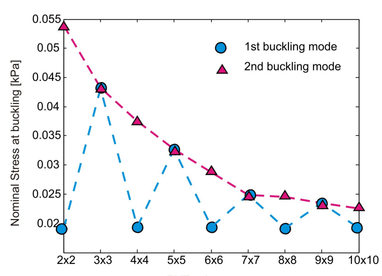

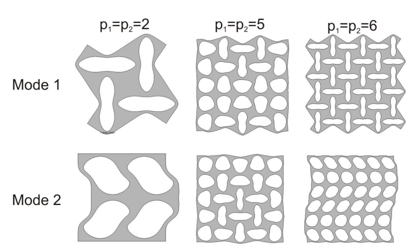

  - All the RVEs with **"even"** primitive cells have the **same 1st Eigen value/ Eigen mode**
  - The **2nd Eigen value decreases** increasing the RVE size, suggesting a **"global" mode**

- **Not rigorous results. Method easy to implement**, helpful to get a first understanding. Rigorous confirmation performing Bloch wave analyses

Saiki I., Terada K. et al., CMAME 2002

34

Lattice structures

There are many examples of cellular materials in nature

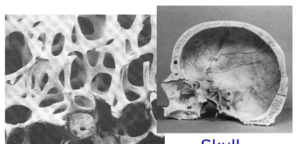

Trabecular bone

Skull

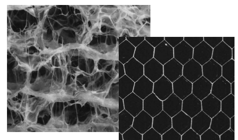

PU foam

Alluminium

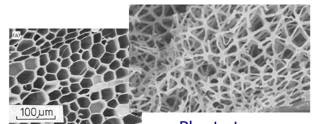

Balsa wood

Plant stem

Gibson, L.J. *J. of Biomechanics*, 2005.

Cellular materials are **mechanically efficient** ➡ high performance

Compression ➡ **nonlinear** stress-strain behavior

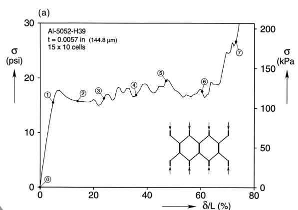

- Initial **instability** (‘yielding’)
- **Elasto-plastic** material
- **Localized deformation** in bands at relatively constant stress

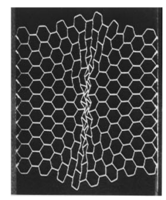

Papka, S.D., Kyriakides, S. *Acta Mater.*, 1998.

35

Post-transformation analysis

Load-displacement analyses for both the **finite-sized and infinite periodic structures** were performed with ABAQUS/Standard thus capturing the post-transformation behavior.

• An **imperfection in the form of the most critical Eigen mode** is introduced into the mesh. The mesh is perturbed by the first Eigen mode ϕ_1, scaled by the scale factor w

$$\Delta x_0 = w\frac{d_x + d_y}{2}\varphi_1.$$

The perturbation Δx_0 introduced into the mesh is a fraction of the averaged center to-center distance between the voids

We used scale factors *w* of 0.05%, 0.1%, 0.5%, and 1%.

For all levels of imperfection the same transformed pattern was obtained.

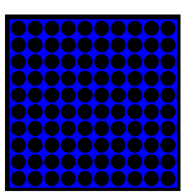

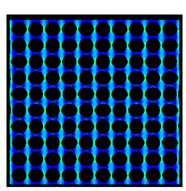

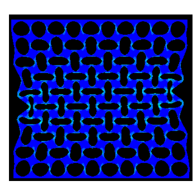

36

Results: Elliptical holes on a rectangular lattice

• **Finite-sized periodic structure** (compression perpendicular to the major axis)

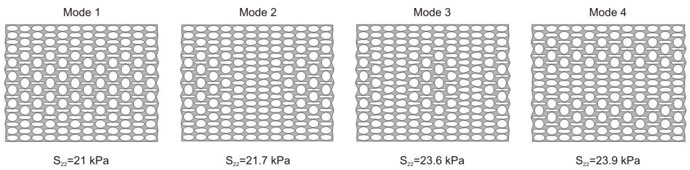

First mode ➡ same pattern as in the experimental test

• **Infinite periodic structure** (compression perpendicular to the major axis)

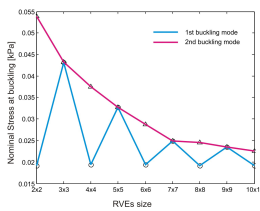

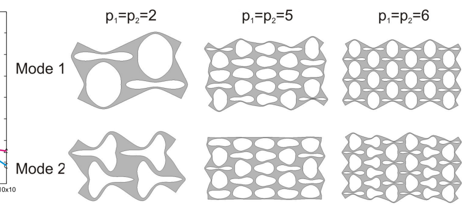

Refined Eigen Analyses

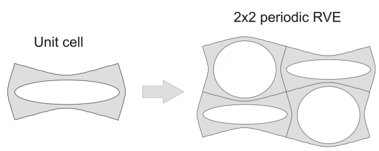

Bloch wave Analyses

• **At instability, enlarged primitive cell pY with p=(2,2)**

• After the 1st Eigen Mode, **loss of ellipticity** occurs

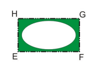

"global" Eigen Mode

37

Results: Elliptical holes on a rectangular lattice

• **Finite-sized periodic structure** (compression parallel to the major axis)

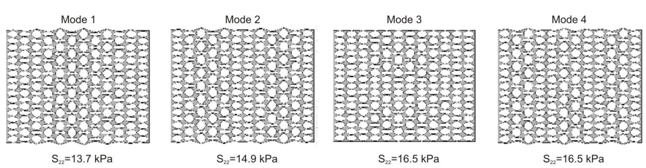

Critical instability strongly influenced by **preloading**

• **Infinite periodic structure** (compression parallel to the major axis)

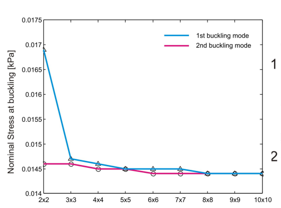

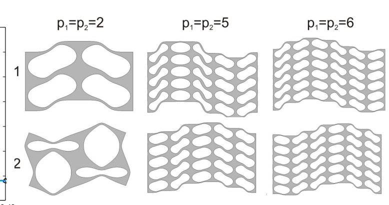

Refined Eigen Analyses

• The first 2 Eigen modes are quite close

• They are independent of the RVE size

"global" Eigen Modes

Bloch wave Analyses

• **No microscopic instability is detected prior to macroscopic instability** (loss of ellipticity)

"global" Eigen Modes

38

Results: Elliptical holes on a rectangular lattice

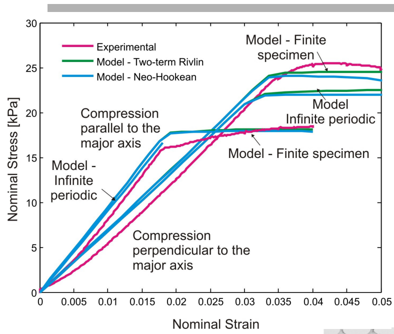

- **Excellent quantitative agreement** between experiments and simulations
- Infinite periodic solid earlier departure from linearity
- For the **two-terms Rivlin and the Neo-Hookean** material models **almost identical** stress-strain behavior

compression perpendicular to the major axis

Experiments

Simulations

compression parallel to the major axis

Experiments

Simulations

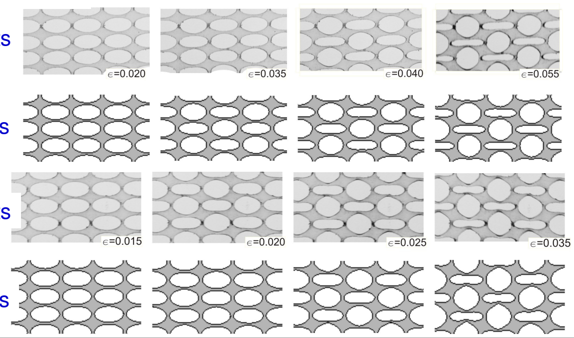

39

Eigen Analysis

$$\int_\Omega \dot{\mathbf{S}} : grad\,\delta\mathbf{v}\,dV - \int_{\partial\Omega} \dot{\mathbf{t}} \bullet \delta\mathbf{v}\,dS = 0,$$

Principle of virtual work in the updated Lagrangian form

1) $\int_\Omega \dot{\mathbf{S}} : grad\,\delta\,\mathbf{v}\,dV = \int_\Omega [\overset{\triangledown}{\boldsymbol{\tau}} : \delta\,\mathbf{D} - \boldsymbol{\tau} : (\delta\mathbf{L}^T\mathbf{L} - 2\,\mathbf{D}\,\delta\,\mathbf{D})]dV,$

where $\delta\,\mathbf{v} = \delta\,\dot{\mathbf{F}} = \delta\,\mathbf{L}$ $\mathbf{D} = \frac{1}{2}(\mathbf{L} + \mathbf{L}^T).$ $\overset{\triangledown}{\tau} = \dot{\tau} - \mathbf{W}\tau + \tau\mathbf{W}$ $\mathbf{S} = \tau\,\mathbf{F}^{-T}$

2) $\dot{\mathbf{t}} = \frac{\partial\,\mathbf{t}}{\partial\,\mathbf{F}} : \dot{\mathbf{F}} = \frac{\partial\,\mathbf{t}}{\partial\,\mathbf{F}} : \mathbf{L}.$ the change in intensities of the applied tractions arises due to the change in geometry

$$\int_\Omega \delta\mathbf{D} : \mathbb{C} : \mathbf{D}\,dV - \int_\Omega (\sigma + \lambda\,\Delta\sigma) : (\delta\mathbf{L}^T\mathbf{L} - 2\,\mathbf{D}\,\delta\,\mathbf{D})dV - \int_{\partial\Omega} \left(\frac{\partial\,(\mathbf{t} + \lambda\,\Delta\mathbf{t})}{\partial\,\mathbf{F}} : \mathbf{L} \right) \bullet \delta\,\mathbf{v}\,dS = \mathbf{0},$$

Finite element discretization $\left(\boldsymbol{K}_0 + \lambda\,\boldsymbol{K}_\Delta\right)\hat{\boldsymbol{v}} = \mathbf{0},$

$\mathbf{K}_0$ is the **initial stiffness matrix** which accounts for the effect of the existing stresses and tractions. $\mathbf{K}_\Delta$ is the **differential stiffness matrix**, generated by the perturbation stresses and tractions.

40

Bloch wave Analysis

Investigation of bifurcations in infinite periodic solids

• **Before bifurcation,** one possible primitive cell Y is identified by the parallelogram
•**At bifurcation,** the initial Y-periodicity may be broken resulting in an enlarged primitive cell **p**Y

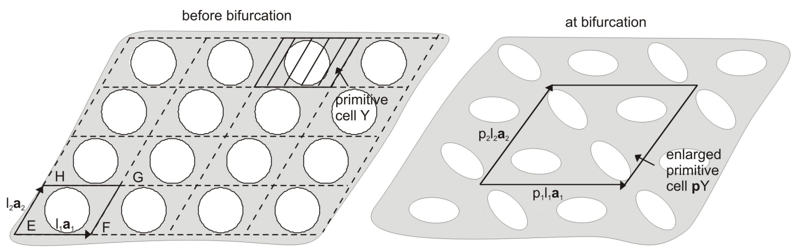

Aberg M., Gudmundson P., J. Acoust. Soc. Am. 1997

Bloch wave Analysis

To obtain the bifurcation modes of the infinite periodic solid

• The primitive Y cell is considered
• The velocities are given by the **Bloch type** relation

$$\mathbf{v}(\mathbf{X}+l_j\,\mathbf{a}_j)=\mathbf{v}(\mathbf{X})\exp[i\mathbf{k}_0\cdot(l_j\,\mathbf{a}_j)],\quad \mathrm{j}=1,2$$

where $\mathbf{k}_0 = k_{01}\mathbf{b}_1 + k_{02}\mathbf{b}_2$ is the wave vector lying in the primitive cell and **v** is in general a complex-valued function

• The velocities and tractions evaluated along opposite sides of the primitive cell are related through

$$\mathbf{v}|_{FG}=d_1\mathbf{v}|_{EH},\quad \mathbf{v}|_{HG}=d_2\mathbf{v}|_{EF},$$

$$\mathbf{v}|_{F}=d_1\mathbf{v}|_{E},\quad \mathbf{v}|_{H}=d_2\mathbf{v}|_{E},\quad \mathbf{v}|_{G}=d_1 d_2\mathbf{v}|_{E},$$

$$\dot{\mathbf{t}}|_{FG}=-d_1\dot{\mathbf{t}}|_{EH},\quad \dot{\mathbf{t}}|_{HG}=-d_2\dot{\mathbf{t}}|_{EF},\qquad d_j=\exp[i\,2\pi\,k_{0j}l_j]$$

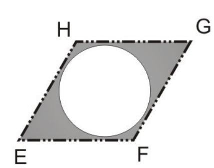

Bloch wave Analysis

ABAQUS does not directly handle complex valued displacements

• All the all of the fields are split into a real and imaginary parts

•Two uncoupled equilibrium equations (one for the real and one for the imaginary part) are obtained

•The problem is solved using two identical finite element meshes for the primitive cell, one for the real part and one for the imaginary part.

•The two meshes are coupled by the displacement boundary conditions given before

•Finite element discretization

$$\begin{bmatrix} K & 0 \\ 0 & K \end{bmatrix} \begin{bmatrix} \hat{v}^{Re} \\ \hat{v}^{Im} \end{bmatrix} = \begin{bmatrix} \dot{f}^{Re} \\ \dot{f}^{Im} \end{bmatrix},$$

• Application of boundary conditions and static condensation of the degrees of freedom belonging to the nodes on the edges HG and FG

$$\tilde{K} \begin{bmatrix} \hat{v}_a^{Re} \\ \hat{v}_a^{Im} \end{bmatrix} = 0,$$

Eigenvalue problem ➡ Find the minimum load for which the lowest eigenvalue is equal to zero

Analysis of instabilities: Loss of ellipticity

Two different types of bifurcation eigenmodes are mapped in the neighborhood of the origin $\mathbf{k}_0=(0, 0)$:

• for $\mathbf{k}_0= \mathbf{0}$ a periodic **"local" mode** is found with $\mathbf{p}=(1,1)$;

• for $\mathbf{k}_0 \to \mathbf{0}$ a **"global" long wavelength mode** is obtained with wavelength much larger than the unit cell size ➡ this corresponds to loss of ellipticity at the macroscopic scale

Loss of ellipticity ➡ response of the macroscopic (homogenized) tangent moduli of the solid

$$\dot{\bar{S}} = \mathbb{L}^H \dot{\bar{F}},$$

Macroscopic instability when

$$\det \mathbf{A}(\mathbf{n})=0$$

where **A(n)** is the acoustic tensor

$$\mathbf{A}(\mathbf{n})\mathbf{g}=\mathbb{L}^H[\mathbf{g} \otimes \mathbf{n}]\mathbf{n}$$

The components of $\mathbb{L}^H$ are identified by subjecting the unit cells to four independent linear perturbations of the macroscopic deformation gradient, calculating the corresponding averaged stress components

44

Wave propagation in periodic materials

Propagation of harmonic waves in a periodic hyperelastic material.

Governing equations

$$\mathrm{Div}\dot{\mathbf{S}} = \rho_0 \frac{\partial^2 \mathbf{V}}{\partial t^2}, \qquad \dot{\mathbf{S}} = \mathbb{L} : \dot{\mathbf{F}}$$

The solution will be in the form

$$\mathbf{V}(\mathbf{X}, t) = \boldsymbol{\mathcal{V}}(\mathbf{X}) \exp[-\mathrm{i}\omega\, t], \quad \Longrightarrow \quad \mathrm{Div}\dot{\boldsymbol{\mathcal{S}}} + \rho_0 \omega^2 \boldsymbol{\mathcal{V}} = 0.$$

complex valued function

The velocities are given by the Bloch type relation

$$\boldsymbol{\mathcal{V}}(\mathbf{X} + l_j \mathbf{a}_j) = \boldsymbol{\mathcal{V}}(\mathbf{X}) \exp[\mathrm{i}\mathbf{K}_0 \cdot (l_j \mathbf{a}_j)].$$

Two sets of uncoupled equations for the real and imaginary parts

$$\begin{cases} \mathrm{Div}\dot{\boldsymbol{\mathcal{S}}}^{Re} + \rho_0 \omega^2 \boldsymbol{\mathcal{V}}^{Re} = 0, \\ \mathrm{Div}\dot{\boldsymbol{\mathcal{S}}}^{Im} + \rho_0 \omega^2 \boldsymbol{\mathcal{V}}^{Im} = 0. \end{cases} \quad \Longleftarrow \quad \begin{array}{l} \boldsymbol{\mathcal{V}}(\mathbf{X} + l_j \mathbf{a}_j)^{Re} = \boldsymbol{\mathcal{V}}^{Re}(\mathbf{X}) \cos[\mathbf{K}_0 \cdot (l_j \mathbf{a}_j)] - \boldsymbol{\mathcal{V}}^{Im}(\mathbf{X}) \sin[\mathbf{K}_0 \cdot (l_j \mathbf{a}_j)] \\ \boldsymbol{\mathcal{V}}(\mathbf{X} + l_j \mathbf{a}_j)^{Im} = \boldsymbol{\mathcal{V}}^{Re}(\mathbf{X}) \sin[\mathbf{K}_0 \cdot (l_j \mathbf{a}_j)] + \boldsymbol{\mathcal{V}}^{Im}(\mathbf{X}) \cos[\mathbf{K}_0 \cdot (l_j \mathbf{a}_j)] \end{array}$$

Aberg M., Gudmundson P., J. Acoust. Soc. Am. 1997

Wave propagation in periodic materials

The problem is solved using two identical finite element meshes for the RVE, one for the real part and one for the imaginary part and coupling them by Bloch type displacement boundary conditions

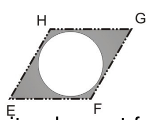

$$\hat{\mathbf{v}} = [\hat{\mathbf{v}}_i \;\; \hat{\mathbf{v}}_a \;\; \hat{\mathbf{v}}_b]^T, \quad \hat{\mathbf{v}}_a = [\hat{\mathbf{v}}_{EF} \;\; \hat{\mathbf{v}}_{EH} \;\; \hat{\mathbf{v}}_E]^T \quad \hat{\mathbf{v}}_b = [\hat{\mathbf{v}}_{HG} \;\; \hat{\mathbf{v}}_{FG} \;\; \hat{\mathbf{v}}_F \;\; \hat{\mathbf{v}}_H \;\; \hat{\mathbf{v}}_G]^T$$

$$\hat{\mathbf{f}} = [\hat{\mathbf{f}}_i \;\; \hat{\mathbf{f}}_a \;\; \hat{\mathbf{f}}_b]^T, \quad \hat{\mathbf{f}}_a = [\hat{\mathbf{f}}_{EF} \;\; \hat{\mathbf{f}}_{EH} \;\; \hat{\mathbf{f}}_E]^T \quad \hat{\mathbf{f}}_b = [\hat{\mathbf{f}}_{HG} \;\; \hat{\mathbf{f}}_{FG} \;\; \hat{\mathbf{f}}_F \;\; \hat{\mathbf{f}}_H \;\; \hat{\mathbf{f}}_G]^T$$

Finite element formulation

$$\left[\begin{pmatrix} [\mathrm{K}] & 0 \\ 0 & [\mathrm{K}] \end{pmatrix} - \omega^2 \begin{pmatrix} [\mathrm{M}] & 0 \\ 0 & [\mathrm{M}] \end{pmatrix} \right] \begin{bmatrix} \hat{\mathbf{v}}^{Re} \\ \hat{\mathbf{v}}^{Im} \end{bmatrix} = \begin{bmatrix} \hat{\mathbf{f}}^{Re} \\ \hat{\mathbf{f}}^{Im} \end{bmatrix}$$

Boundary conditions yield

$$\begin{bmatrix} \hat{\mathbf{v}}^{Re} \\ \hat{\mathbf{v}}^{Im} \end{bmatrix} = [\mathrm{Q}_v] \begin{bmatrix} \hat{\mathbf{v}}_i^{Re} \\ \hat{\mathbf{v}}_a^{Re} \\ \hat{\mathbf{v}}_i^{Im} \\ \hat{\mathbf{v}}_a^{Im} \end{bmatrix} \qquad \begin{bmatrix} \hat{\mathbf{f}}^{Re} \\ \hat{\mathbf{f}}^{Im} \end{bmatrix} = [\mathrm{Q}_f] \begin{bmatrix} \hat{\mathbf{f}}_i^{Re} \\ \hat{\mathbf{f}}_a^{Re} \\ \hat{\mathbf{f}}_i^{Im} \\ \hat{\mathbf{f}}_a^{Im} \end{bmatrix}$$

$$\boxed{[\mathrm{Q}_v]^T \left[\begin{pmatrix} [\mathrm{K}] & 0 \\ 0 & [\mathrm{K}] \end{pmatrix} - \omega^2 \begin{pmatrix} [\mathrm{M}] & 0 \\ 0 & [\mathrm{M}] \end{pmatrix} \right] [\mathrm{Q}_v] \begin{bmatrix} \hat{\mathbf{v}}_i^{Re} \\ \hat{\mathbf{v}}_a^{Re} \\ \hat{\mathbf{v}}_i^{Im} \\ \hat{\mathbf{v}}_a^{Im} \end{bmatrix} = 0}$$

Wave propagation in periodic materials

Step 1: Undeformed RVE

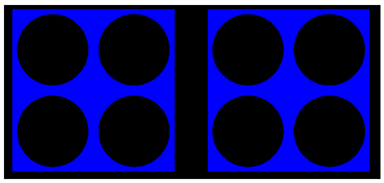

Step 2: Deformed RVE

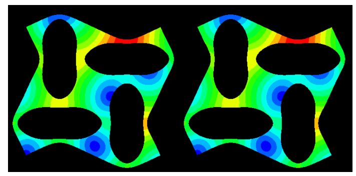

Step 3: EigenFrequency analysis

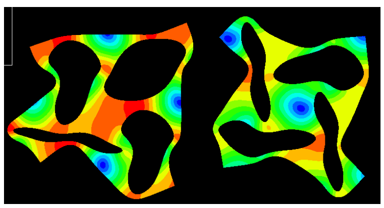

Mode1

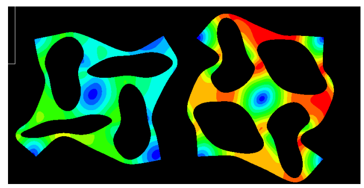

Mode2

Effects of inclusions

Square lattice of circular holes

+

Inclusions

- **Cotton balls (~constant density)**
- **Different inclusions patterns**

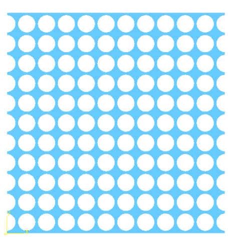

Goal

- **to obtain specified pattern transformations trough the use of strategically placed inclusions**

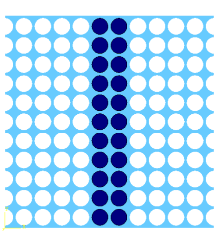

Vertical inclusions

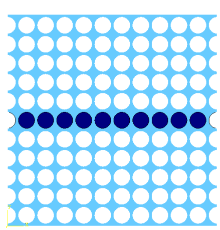

Horizontal inclusions

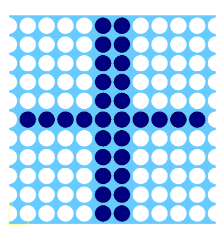

Cross inclusions

Vertical inclusions

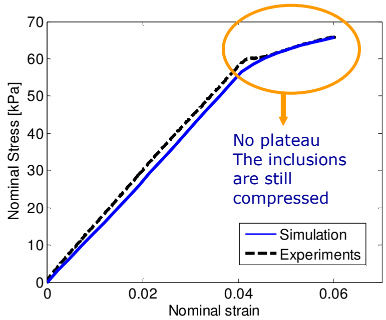

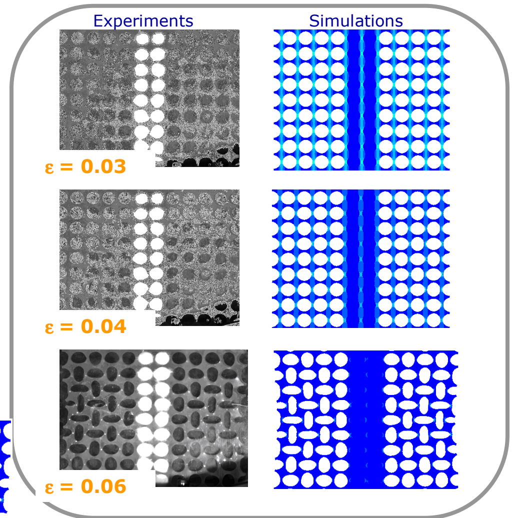

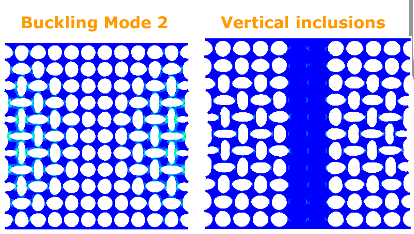

Vertical Inclusions

- **Suppress mode 1 in favor of Mode 2**

Horizontal inclusions

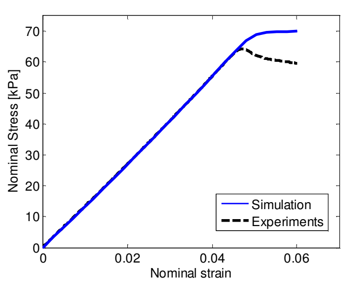

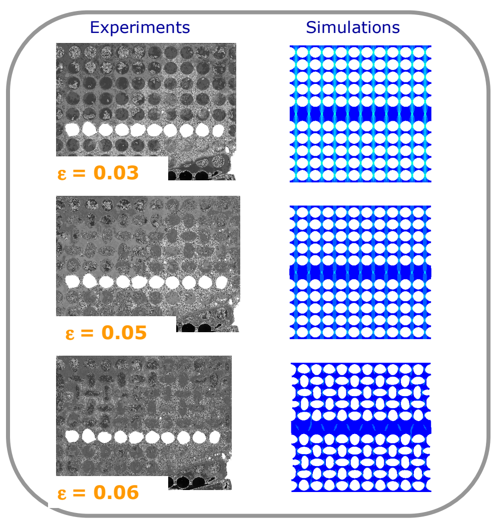

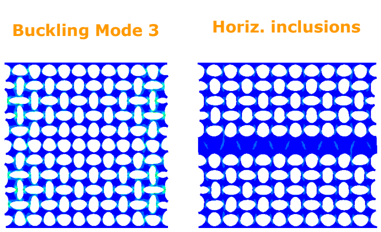

Horizontal Inclusions

- **Suppress mode 1 in favor of Mode 3**

Cross inclusions

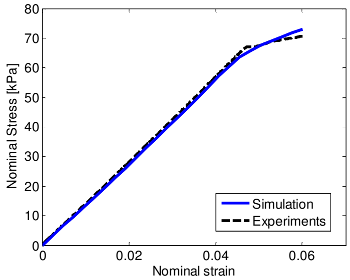

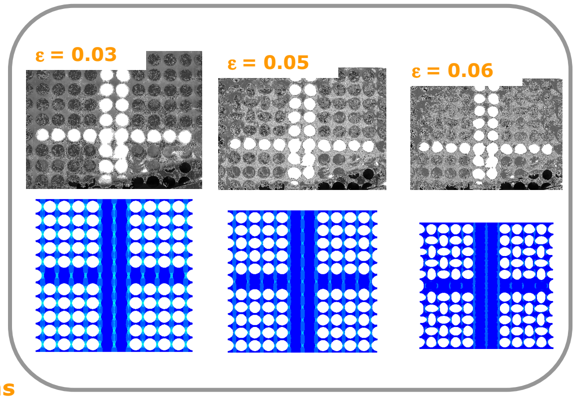

Horizontal & Cross Inclusions

- **numerical** model shows **symmetric** pattern transformation
- the **experimental** results show pattern transformation **in small localized area**

- inclusions act as a barrier
- the **system is not truly symmetric in the experimental setup** (the very bottom of the structure is not as free to deform)
- **Solution:** Larger lattice will lessen the effects of the boundary conditions

Combining cases

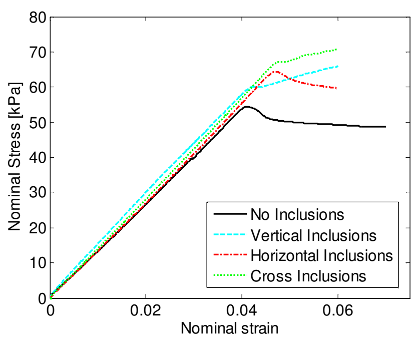

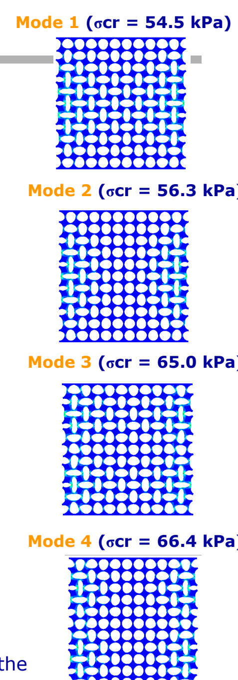

- The **linear elastic regime** remains the same in all cases
- The **critical buckling load** is different for each case
- The order in which the load increases follows the order of the buckling mode that each case is trying to mimic.
- Both the **vertical and cross cases** show a **non-zero slope after buckling** occurs that results from the ongoing stiffness contribution from the compression of the inclusions.

Constitutive model

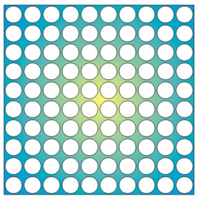

Constitutive model for the overall response of periodic porous elastomers

- Use the constitutive model to capture the instabilities

Work in progress….

RVE **Macroscopic deformation**

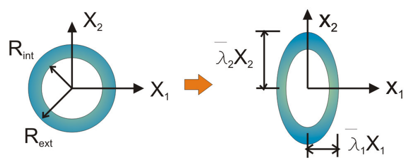

$$\overline{\mathbf{F}} = \overline{\lambda}_1\, \mathbf{e}_1 \otimes \mathbf{e}_1 + \overline{\lambda}_2\, \mathbf{e}_2 \otimes \mathbf{e}_2.$$

Deformation fields

$$x_i = \psi_i(R)\, X_i \qquad F_{ij} = \frac{\partial \mathbf{x}_i}{\partial \mathbf{X}_j} = \frac{\partial \psi_i}{\partial R}\frac{X_i X_j}{R} + \psi_i \delta_{ij}$$

Incompressibility det J=1

$$\frac{\partial \psi_1}{\partial R}\psi_2 - \frac{\partial \psi_2}{\partial R}\psi_1 = 0, \qquad \psi_1\, \psi_2 + R\, \psi_1 \frac{\partial \psi_2}{\partial R} = 1.$$

$$\Rightarrow \quad \psi_1(R) = c_1\, \psi(R), \qquad \psi_2(R) = \frac{1}{c_1}\, \psi(R),$$

$$\Rightarrow \quad \psi(R) = \sqrt{1 + \frac{c_2^2}{R^2}}, \qquad c_1 = \sqrt{\frac{\overline{\lambda}_1}{\overline{\lambda}_2}}, \quad c_2 = R^+\sqrt{\overline{J}-1},$$

53

Constitutive model

Incompressible Neo-Hookean material

Homogenized strain energy

$$\overline{W}_{NH} = \frac{\mu}{4\,\overline{J}}\left[2(1-f_0)(\overline{I}_1 - 2\overline{J}) + (\overline{J}-1)\overline{I}_1 \log\left(\frac{f_0 - 1 + \overline{J}}{\overline{J}\, f_0}\right)\right].$$

Macroscopic stress

$$\overline{\boldsymbol{\sigma}} = \frac{\mu}{2\,\overline{J}^2}\left[2(1-f_0) + (\overline{J}-1)\log\left(\frac{f_0 - 1 + \overline{J}}{\overline{J}\, f_0}\right)\right]\overline{\mathbf{B}} + \frac{\mu\,\overline{I}_1}{4\,\overline{J}^2}\left[(1-f_0)\frac{2f_0 - 1 + \overline{J}}{f_0 - 1 + \overline{J}} + \log\left(\frac{f_0 - 1 + \overline{J}}{\overline{J}\, f_0}\right)\right]\mathbf{I}.$$

Equibiaxial loading

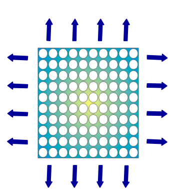

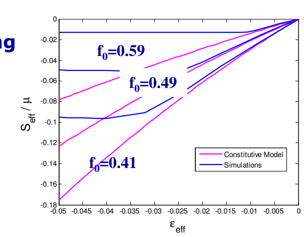

Compression

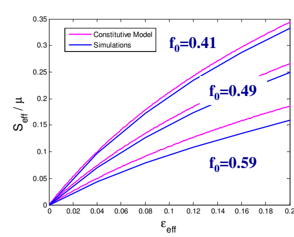

Tension

Work in progress….

54